ACS OMEGA

http://pubs.acs.org/journal/acsodf

Article

Pd(II)-Imprinted Chitosan Adsorbent for Selective Adsorption of Pd(II): Optimizing the Imprinting Process through Box−Behnken Experimental Design

Shuo Lin, Wei Wei, Xiaoyu Lin, John Kwame Bediako, D. Harikishore Kumar Reddy, Myung-Hee Song,* and Yeoung-Sang Yun*

Cite This: *ACS Omega* 2021, 6, 13057−13065

Read Online

ACCESS | Metrics & More | Article Recommendations | Supporting Information

ABSTRACT: The ion/molecular imprinting technique is an efficient method for developing materials with high adsorption selectivity. However, it is still difficult to obtain an imprinted adsorbent with desirably high selectivity when the preparation processes are not well designed and optimized. In this present work, a chitosan-based ion-imprinted adsorbent was optimally prepared through Box−Behnken experimental design to achieve desirably high selectivity for Pd anions ($PdCl_4^{2-}$) from aqueous solutions with high acidity. The dosage of epichlorohydrin (ECH) used in the first and second steps of cross-linking as well as the pH of the imprinting reaction medium is likely one of the key factors affecting the selectivity of the synthesized ion-imprinted chitosan adsorbent, which were selected as factors in a three-level factorial Box−Behnken design. As a result, the effects of these three factors on Pd(II) selectivity were able to be described by using a second-order polynomial model with a high regression coefficient (R^2; 0.996). The obtained optimal conditions via the response surface methodology were 0.10% (v/v) of first cross-linking ECH, an imprinting pH of 1.0, and 1.00% of second cross-linking ECH. Competitive adsorption was performed to investigate the selectivities of the ion-imprinted chitosan adsorbents prepared under the optimal conditions. The selectivity coefficient of Pd(II) versus Pt(IV) ($\beta_{Pd/Pt}$) of the Pd(II)-imprinted adsorbent was 115.83, much greater than that of the chitosan adsorbent without imprinting and various reported selective adsorbents. Therefore, the Box−Behnken design can be a useful method for optimizing the synthesis of ion-imprinted adsorbents with desirably high adsorptive selectivity for precious metals.

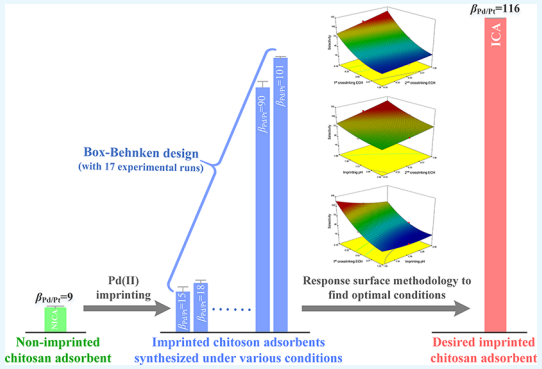

INTRODUCTION

Platinum group metals (PGMs) as marvelous metallic materials show wide utilization in various industries, including applications in photography, jewelry, dentistry, hydrogen storage, electronics, and catalysts.[1,2] The increasing commercial values of PGMs have prompted focus on their recovery from secondary sources, such as inactivated catalysts and electronic devices.[3−5] Generally, PGMs are dissolved in acids through reaction with chlorine solution and transformed to be anionic metal species such as $PdCl_4^{2-}$ and $PtCl_6^{2-}$ in hydrometallurgical processes. Conventional methods for recovering dissolved metal ions in hydrometallurgical processes, such as ion exchange, reverse osmosis, co-precipitation, solvent extraction, and membrane filtration,[4,6] have significant shortcomings, which include generating toxic byproducts, extensive costs of labor, large energy requirements, high doses of reagents, or low recovery efficiency or selectivity. Fortunately, adsorption is believed to be one of the most promising alternative techniques for separation and extraction of PGMs without the aforementioned disadvantages.

Chitosan, an easy-to-obtain and price-moderate biopolymeric derivative, is well known as a high-potential adsorbent for metal recovery owing to its abundant amine groups, which can electrostatically attract or complex with metallic anions or cations, respectively.[7−9] Nevertheless, the poor acid stability and insignificant selectivity of chitosan in multiple-metal solutions impede its practical applications. Therefore, several studies of precious metal adsorption on chitosan aimed to improve its stability at low pH and selectivity for target metals.[10−12]

Ion imprinting is effective for developing adsorbents with high selectivities for target ions.[13,14] Taking the ion-imprinted chitosan adsorbent for example, the ion-imprinting technique

Received: February 5, 2021
Accepted: April 29, 2021
Published: May 12, 2021

Scheme 1. Concept of the Cross-Linking and Imprinting Processes

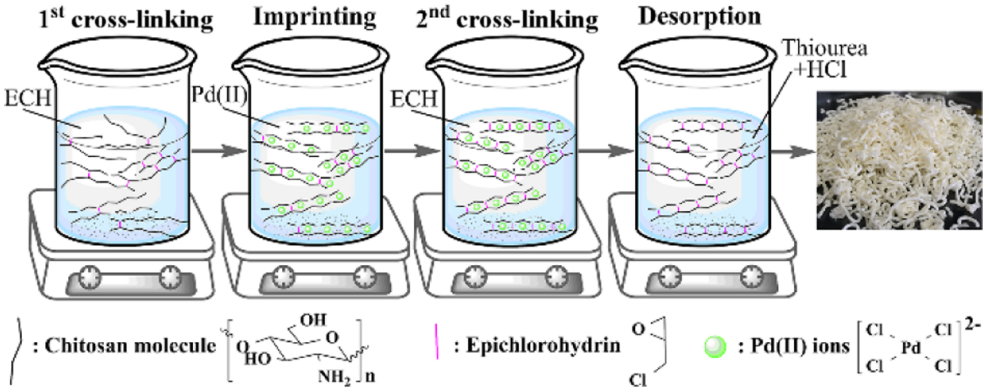

involves the following steps (Scheme 1): (i) chitosan materials in a shape body react with cross-linkers to obtain enough stability for subsequent steps, (ii) the resultant chitosan materials are mixed with template ions to form specific adsorptive bindings, (iii) the template-loaded chitosan materials react with the cross-linker again to fix the specific binding environments in the adsorbents, and (vi) the template ions are removed from the chitosan materials.[15,16] After imprinting, the imprinted chitosan adsorbent (ICA) reserves an appropriate size of binding space and a specific binding site that are able to accommodate and bind a specific ion, which contributes to its recognition/selectivity for the target ion.[17,18]

Recently, a great deal of attention has focused on adopting ion-imprinting methods to prepare selective adsorbents for heavy metals,[19−21] including our previous study: an ion-imprinted chitosan fiber synthesized via twice of cross-linking and Pd imprinting.[16] However, the preparation of an ion-imprinted adsorbent generally needs many steps as aforementioned, and the conditions in each step can significantly affect the selective performance of the resultant adsorbent. To ensure desirably high selectivity toward the target Pd(II) ions, the response surface methodology (RSM), which explores the relationships among several explanatory and response variables to determine the optimal response,[22−24] was applied to figure out the optimal conditions for the synthesis of the ion-imprinted adsorbent. In this work, the dosage of epichlorohydrin (ECH) used in the first and second steps of cross-linking as well as the pH of the imprinting reaction medium is likely one of the key factors affecting the selectivity of the synthesized ion-imprinted chitosan adsorbent, which were selected as factors in a three-level factorial Box−Behnken experimental design, which is considered to be more proficient and most powerful than other designs such as the three-level full factorial design, central composite design, and Doehlert design.[25] RSM successfully verified the effect of these major factors on the adsorbent's selectivity. The optimal conditions were determined and employed to prepare a desirably high-selective adsorbent for Pd(II) from acidic solutions.

MATERIALS AND METHODS

Materials. PGM salts ($PdCl_2$ and $H_2PtCl_6{\cdot}5.5H_2O$) were purchased from Kojima Chemicals Co., Ltd. (Sayama, Japan). Three commercial ion-exchange resins, Amberlite IR-120H (IR-120H), Amberjet 4200 (IR-4200), and Amberlite IRA-900 (IR-900); heavy metal salts [$Co(NO_3)_2{\cdot}6H_2O$ and $NiSO_4{\cdot}6H_2O$]; chitosan (75−85% deacetylated); ECH; and thiourea were obtained from Sigma-Aldrich (Yongin, Korea).

Adsorbent Synthesis. The ion-imprinted chitosan adsorbent was synthesized using a method reported previously.[16] In brief, a chitosan solution (5 g of powder-form chitosan was fully dissolved in 100 mL of 3% (v/v) acetic acid aqueous solution) was extruded through the spinneret (0.25 mm inner diameter) into 1 M NaOH solution for coagulating into a fibrous form and then separated for subsequent steps. As illustrated in Scheme 1, (i) the first cross-linking was performed by reacting 2.0 g of undried chitosan fibers with 25 mL of ECH solution (0.10, 0.55, and 1.00 v/v %; the molar ratios of ECH to the chitosan monomer are 0.5:1, 2.75:1, and 5:1, respectively) under alkaline conditions (pH 12.5) at 40 °C for 4 h and then filtrated out and washed for the imprinting process; (ii) the cross-linked fibers were contacted for 12 h with 40 mL of Pd(II) solution (1200 mg L^{-1}), which was prepared by dissolving $PdCl_2$ in HCl solution (pH 1.0, 1.7, and 2.4, 25 °C; slightly cross-linked chitosan could fully dissolve in solution with pH below 1.0); (iii) further cross-linking was conducted for 6 h using 40 mL of ECH solution (0.10, 0.55, and 1.00 v/v %); and (iv) the Pd(II) template was completely eluted from the ion-imprinted chitosan fibers by 0.2 M thiourea solution (in 0.05 M HCl solution). The resultant Pd(II)-imprinted chitosan adsorbent, labeled as ICA, was washed with an alkaline solution and distilled water and then dried in a freeze dryer.

Non-ICA (NICA) was synthesized following an identical process to ICA but without imprinting.

Competitive Adsorption Experiments. The selective performances of the prepared adsorbents were evaluated by adsorption experiments, which were carried out at 25 °C and 150 rpm in a multishaking incubator with 0.01 g of adsorbents in 25 mL of the multiple-metal solution containing metal ions of Co(II), Ni(II), Pt(IV), and Pd(II). This solution was prepared by dissolving metal salts of $Co(NO_3)_2{\cdot}6H_2O$, $NiSO_4{\cdot}6H_2O$, $PdCl_2$, and $H_2PtCl_6{\cdot}5.5H_2O$ in 0.1 M HCl solution with an initial concentration of 200 mg L^{-1} for each metal ion. The pH of the solutions during the 24 h adsorption period were maintained at 1.0. After reaching the equilibrium, the concentration of metal ions in the supernatant was determined after appropriate dilution by inductively coupled plasma-optical emission spectrometry (ICP-OES), and the metal uptakes on the adsorbents (q, mg g^{-1}) were determined by eq 1

$$q = \frac{(C_i - C_e)V}{m} \quad (1)$$

https://doi.org/10.1021/acsomega.1c00685
ACS Omega 2021, 6, 13057−13065

where C_i and C_e are the initial and equilibrium metal concentrations (mg L^{-1}), respectively; V is the solution volume (L); and m is the mass of an adsorbent (g). The selectivity coefficient (β) was introduced to evaluate the adsorbent's selectivity for Pd(II) toward a competing metal ion[26,27]

$$\beta_{\mathrm{Pd/competitive\ metal}} = \frac{K_{\mathrm{Pd}}}{K_{\mathrm{competitive\ metal}}} = \frac{q_{\mathrm{Pd}}}{C_{\mathrm{e(Pd)}}} \div \frac{q_{\mathrm{competitive\ metal}}}{C_{\mathrm{e(competitive\ metal)}}} \quad (2)$$

where K_{Pd} and $K_{\mathrm{competitive\ metal}}$ are the distribution coefficients (L g^{-1}) of Pd and a competitive metal, respectively.

Box–Behnken Design. In Box–Behnken design, the dosage of ECH used in the first and second steps of cross-linking and the pH of the imprinting reaction were selected as independent variables. The real values of three factors coded as −1, 0, and +1 were set at low, center, and high levels, respectively (Table 1). The selectivity coefficient value of Pd versus Pt ($\beta_{\mathrm{Pd/Pt}}$) was chosen as the dependent variable. Therefore, the input factors were ECH concentrations used in the first (X_1) and second (X_3) cross-linking and imprinting pH (X_2) values. The three-factorial Box–Behnken design was performed with 17 runs with 5 center points (Table 2).

Table 1. Experimental Ranges and Levels of the ECH Dosages of the First (X_1) and Second Cross-Linking (X_3) and Imprinting pH (X_2)

independent variables	range and level		
	low (−1)	center (0)	high (+1)
first cross-linking ECH, % (X_1)	0.10	0.55	1.00
imprinting pH (X_2)	1.0	1.7	2.4
second cross-linking ECH, % (X_3)	0.10	0.55	1.00

Instruments. Fourier transform infrared (FTIR) spectroscopy (FT/IR-300E, JASCO, Japan) and X-ray photoelectron spectroscopy (XPS; JSM-6400, JEOL, Japan) were performed to verify the species of Pd(II) loaded on the chitosan adsorbent and the functional groups responsible for Pd(II) imprinting. The metal concentrations were determined by ICP-OES (ICAP-7500, Shimadzu, Japan).

RESULTS AND DISCUSSION

Box–Behnken Statistical Analysis. Based on the Box–Behnken design matrix in Table 2, Design Expert (v8.0; Stat-Ease, Inc.) suggested that a quadratic model is most suitable for fitting experimental results (Table S1). As shown in the analysis of variance (ANOVA) table (Table 3), these very low "Prob > F" values (less than 0.05) for the "Model" and the model terms of X_1, X_2, X_3, X_1X_2, X_1X_3, X_2X_3, X_1^2, and X_2^2 indicated that the model and these model terms were significant. Meanwhile, the insignificance for "Lack of fit" with a high value of "Prob > F" (0.4132)" implied that the model was fit. Thereafter, the final equations in terms of actual factors (first cross-linking: FC; imprinting pH: IpH; and second cross-linking: SC) and coded factors (X_1, X_2, and X_3) can be represented as the following:

$$\begin{aligned}\text{selectivity} = {} & 142.12 - 195.88\mathrm{FC} - 59.13\mathrm{IpH} + 49.87\mathrm{SC} \\ & + 27.52\mathrm{FC} \times \mathrm{IpH} - 39.30\mathrm{FC} \times \mathrm{SC} \\ & - 12.56\mathrm{IpH} \times \mathrm{SC} + 92.13\mathrm{FC}^2 + 11.90\mathrm{IpH}^2 \\ & + 4.60\mathrm{SC}^2 \end{aligned} \quad (3)$$

$$\begin{aligned} Y = {} & 27.06 - 31.21X_1 - 7.31X_2 + 5.39X_3 + 8.67X_1X_2 \\ & - 7.96X_1X_3 - 3.96X_2X_3 + 18.66{X_1}^2 + 5.83{X_2}^2 \\ & + 0.93{X_3}^2 \end{aligned} \quad (4)$$

The regression coefficient (R^2) of the model was 0.996 (Table 3), revealing that eqs 3 and 4 are able to represent the system under the chosen experimental ranges. Moreover, the

Table 2. Box–Behnken Design Matrix with Three Independent Variables for the Experimental and Predicted Pd Selectivity Coefficient Values

	independent variables						dependent variable	
	coded values			real values			selectivity coefficient	
run	X_1	X_2	X_3	ECH (%)	pH	ECH (%)	β_{exp}	β_{pred}
1	−1	−1	0	0.10	1.0	0.55	100.98 ± 0.70	98.74
2	+1	−1	0	1.00	1.0	0.55	18.04 ± 1.21	18.97
3	−1	+1	0	0.10	2.4	0.55	67.71 ± 0.17	66.78
4	+1	+1	0	1.00	2.4	0.55	19.45 ± 0.94	21.69
5	−1	0	−1	0.10	1.7	0.10	62.42 ± 2.03	64.51
6	+1	0	−1	1.00	1.7	0.10	19.09 ± 0.06	18.00
7	−1	0	+1	0.10	1.7	1.00	90.12 ± 2.36	91.21
8	+1	0	+1	1.00	1.7	1.00	14.96 ± 1.83	12.87
9	0	−1	−1	0.55	1.0	0.10	31.63 ± 2.35	31.78
10	0	+1	−1	0.55	2.4	0.10	26.23 ± 0.15	25.07
11	0	−1	+1	0.55	1.0	1.00	49.32± 1.20	50.48
12	0	+1	+1	0.55	2.4	1.00	28.10 ± 0.71	27.95
13	0	0	0	0.55	1.7	0.55	28.12 ± 0.41	27.06
14	0	0	0	0.55	1.7	0.55	24.72 ± 1.85	27.06
15	0	0	0	0.55	1.7	0.55	27.23 ± 0.56	27.06
16	0	0	0	0.55	1.7	0.55	26.91 ± 0.42	27.06
17	0	0	0	0.55	1.7	0.55	28.31 ± 2.10	27.06

https://doi.org/10.1021/acsomega.1c00685
ACS Omega 2021, 6, 13057−13065

Table 3. ANOVA for the Quadratic Model[a]

source	sum of squares	df	mean square	F-value	prob > F	
model	10753.51	9	1194.83	247.10	<0.0001	significant
X_1-first cross-linking	7793.14	1	7793.14	1611.66	<0.0001	
X_2-imprinting pH	427.49	1	427.49	88.41	<0.0001	
X_3-second cross-linking	232.52	1	232.52	48.09	0.0002	
X_1X_2	300.68	1	300.68	62.18	<0.0001	
X_1X_3	253.29	1	253.29	52.38	0.0002	
X_2X_3	62.57	1	62.57	12.94	0.0088	
X_1^2	1465.65	1	1465.65	303.10	<0.0001	
X_2^2	143.10	1	143.10	29.59	0.0010	
X_3^2	3.66	1	3.66	0.76	0.4132	
residual	33.85	7	4.84			
lack of fit	25.64	3	8.55	4.16	0.1010	not significant
pure error	8.21	4	2.05			
Cor total	10,787.35	16				

[a] R^2 = 0.996, pred. R^2 = 0.961, adj. R^2 = 0.993.

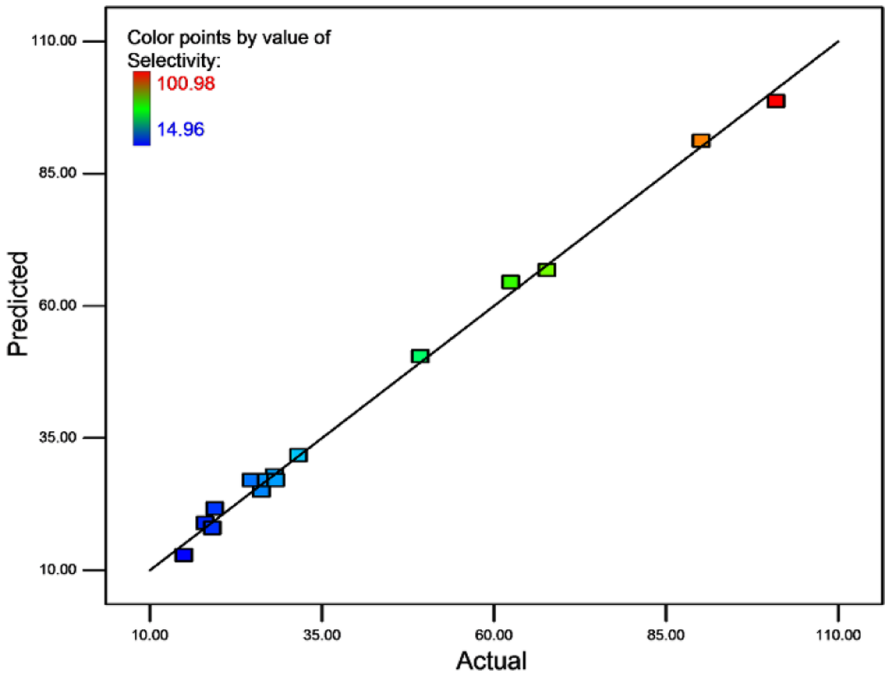

Figure 1. Plot of actual and predicted selectivity coefficient values.

actual and predicted Pd(II) values of selectivity coefficient are listed in Table 2 and Figure 1. The actual selectivities (β_{exp}) were the experimental data obtained under designated conditions, and the predicted selectivities (β_{pred}) were determined using eq 3. As listed in Table 3, the "predicted R^2" of 0.961 was consistent with the "adjusted R^2" of 0.993, indicating the successful description of the actual Pd selectivity coefficient values by eq 3.

The three-dimensional (3-D) response surface plots for the selectivity coefficient as a measured response were obtained based on eq 3 (Figure 2). Figure 2a showed the 3-D response surface relationship between first cross-linking ECH and imprinting pH on the selectivity coefficient at the high level of the second cross-linking ECH (1.00%). The selectivity increased as the first cross-linking ECH dosage and the imprinting pH decreased. The 3-D response surface relationship between first cross-linking ECH and second cross-linking ECH on the selectivity coefficient at the low level of the imprinting pH (1.0) is shown in Figure 2b. The trend for first cross-linking ECH was the same as that in Figure 2a. The selectivity increased as the second cross-linking ECH dosage increased. Figure 2c displays a 3-D response surface between imprinting pH and second cross-linking ECH on the selectivity coefficient at the low level of the first cross-linking ECH (0.10%). The trends for imprinting pH and second cross-linking ECH were identical to those in Figure 2a,b, respectively.

The first cross-linking was conducted to impart a degree of chemical stability on the chitosan fibers before imprinting to prevent their dissolution in the extremely acidic Pd(II) imprinting solution. However, excessive cross-linking would impede reassembly of the template ions and functional groups on chitosan, leading to the ICA having lower selectivity for the target Pd(II) ions. Thus, the selectivity coefficient markedly increased as the dosage of ECH in the first cross-linking decreased (as seen in Figure 2a,b). In contrast, a sufficiently

https://doi.org/10.1021/acsomega.1c00685
ACS Omega 2021, 6, 13057−13065

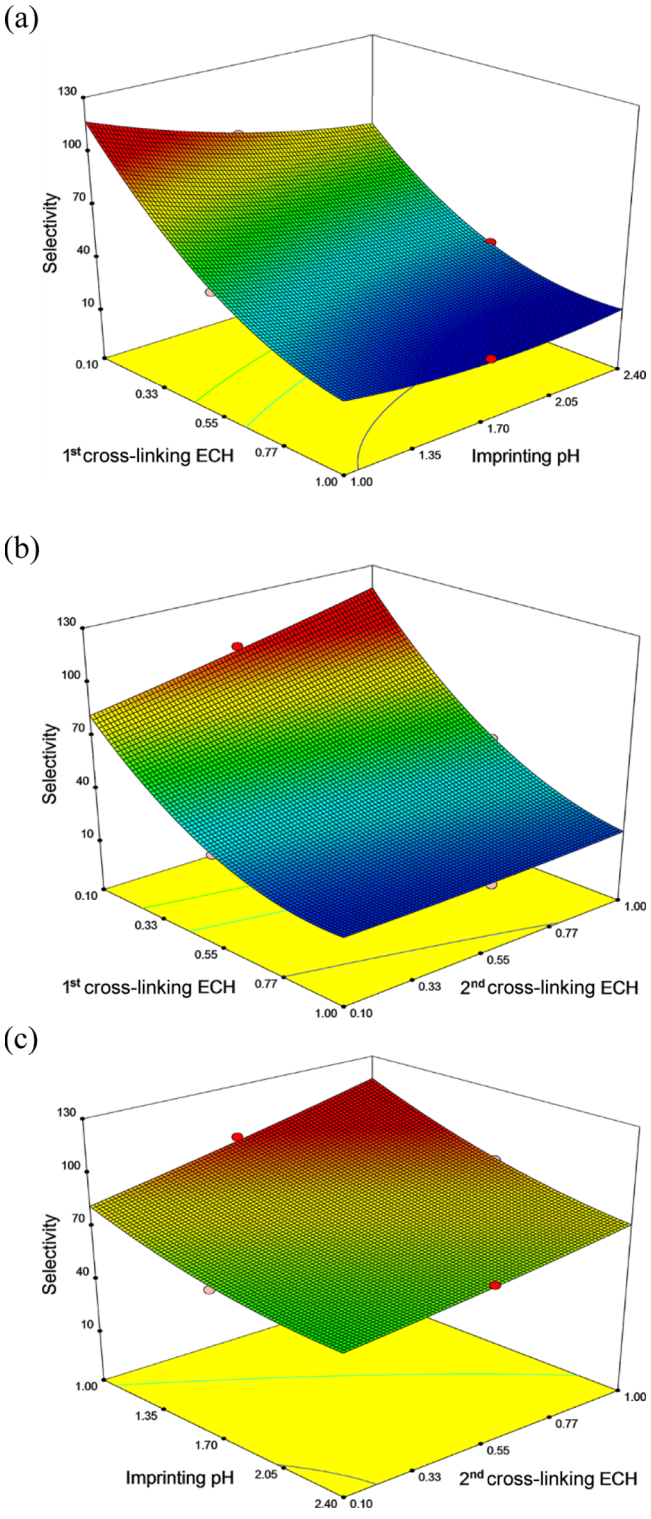

Figure 2. Response surface plots illustrating (a) effects of first cross-linking ECH (X_1) and imprinting pH (X_2) on the selectivity coefficient at the high level of the second cross-linking ECH (X_3), (b) effects of first cross-linking ECH (X_1) and second cross-linking ECH (X_3) on the selectivity coefficient at the low level of the imprinting pH (X_2), and (c) effects of imprinting pH (X_2) and second cross-linking ECH (X_3) on the selectivity coefficient at the low level of the first cross-linking ECH (X_1).

high degree of cross-linking (second cross-linking) after imprinting would fix the chemical structure formed by

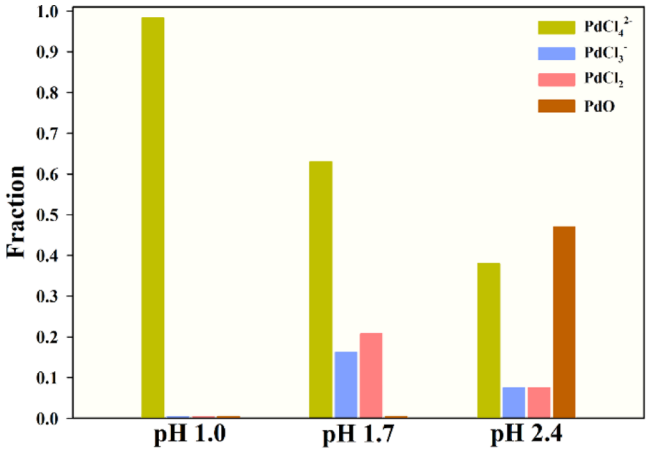

Figure 3. Fractions of Pd species in 1200 mg L^{-1} Pd(II) solutions: $PdCl_2$ was dissolved in diluted hydrochloric acid at pH 1.0, 1.7, and 2.4.

imprinting, which is primarily responsible for the recognition/selectivity for the target ions of ICA. Thus, when the dosage of ECH in the second cross-linking increased, the selectivity increased (as seen in Figure 2b,c)

Additionally, the reason that a lower imprinting pH resulted in a higher Pd(II) selectivity is because the presence of Pd(II) species depends significantly on the solution pH, and during imprinting, the functional groups on chitosan showed the highest affinity for $PdCl_4^{2-}$. The simulated fraction of Pd(II) species in solution was obtained by the Medusa program (Royal Institute of Technology, Sweden). As shown in Figures 3 and S1, all Pd(II) existed as $PdCl_4^{2-}$ in solution at pH 1.0, and 63.0% of Pd(II) existed as $PdCl_4^{2-}$ in solution at pH 1.7; meanwhile, in a pH 2.4 solution, 38.0% of $PdCl_4^{2-}$ coexisted with $PdCl_3^-$ (7.5%), $PdCl_2$ (7.5%), and PdO (47.0%). Hence, the Pd(II) solution at pH 1.0 supplied a greater quantity of $PdCl_4^{2-}$ for imprinting. Additionally, the Pd(II) species loaded in/on chitosan fibers and the functional groups were investigated by XPS analysis after imprinting. The XPS analysis for Pd 3d, Cl 2p, and N 1s of chitosan fibers imprinted at pH 1.0, 1.7, and 2.4, respectively, was performed (Figure 4). The Pd 3d peaks with binding energies at 338.2 and at 336.4 eV could be assigned to $PdCl_4^{2-}$ for imprinting at pH 1.0 and 1.7 and PdO for imprinting at pH 2.4, respectively.[28−32] The Cl 2p spectra of chitosan imprinted at pH 1.0 and 1.7 consist of doublets at 198.5 eV (Cl $2p_{3/2}$) and 200.1 eV (Cl $2p_{1/2}$), which could be assigned to Cl in the complex of $PdCl_4^{2-}$ (Pd−Cl).[32−34] However, a new doublet at 197.6 and 199.1 eV, assigned to Cl^-, was observed for the spectrum of chitosan imprinted at pH 2.4. The N 1s peaks with the binding energies at 402.1, 400.6, and 398.8 eV could be assigned to Pd-loaded $-NH_3^+$, $-NH_3^+$, and $-NH_2$ amine groups, respectively.[32,35−37] The XPS results confirmed that in solution at pH 1.0, amine groups bound with $PdCl_4^{2-}$ for imprinting, as shown in eq 5 and Figure S2, where "C" denotes the chitosan backbone

$$2C-(NH_3^+)_n + nPdCl_4^{2-} \rightarrow C-(NH_3^+ \cdot PdCl_4^{2-} \cdot {}^-H_3N)_n-C \quad (5)$$

When conducting the Pd imprinting at pH 2.4, only PdO could be found in the chitosan fibers. Therefore, the binding between $PdCl_4^{2-}$ and protonated amine groups in/on chitosan made the greatest contribution to Pd(II) imprinting.

https://doi.org/10.1021/acsomega.1c00685
ACS Omega 2021, 6, 13057−13065

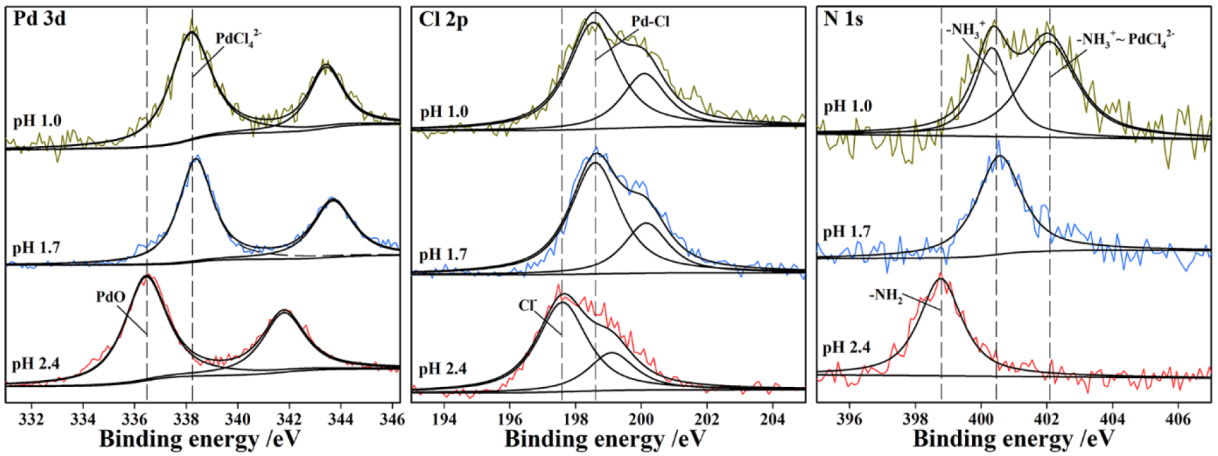

Figure 4. XPS Pd 3d, Cl 2p, and N 1s spectra of chitosan fibers imprinted at pH 1.0, 1.7, and 2.4, respectively.

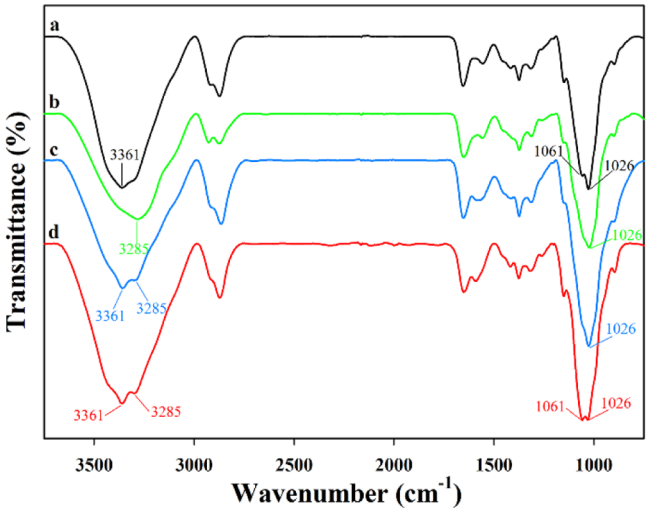

Figure 5. FTIR spectra of (a) NICA, (b) chitosan fibers after imprinting at pH 1.0, (c) chitosan fibers after second cross-linking (final pH 7.5), and (d) prepared ICA.

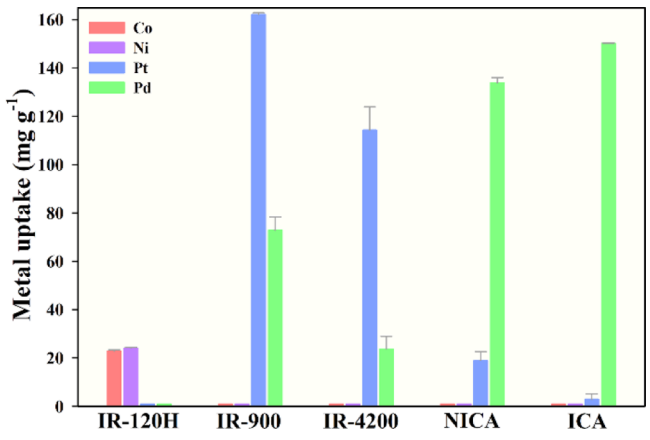

Figure 6. Metal uptakes on the adsorbents (IR-120H, IR-900, IR-4200, NICA, and ICA) in a multiple-metal solution containing Co(II), Ni(II), Pt(IV), and Pd(II).

Notably, a higher pH facilitates cross-linking of chitosan with ECH (Figure S3);[38] however, it could also affect the imprinted Pd species as previously proved. Thus, three samples of Pd-imprinted chitosan fibers were prepared by adjusting the pH of the second cross-linking solution to 7.5, 12.5, and 14.5, and the species of the imprinted Pd(II) retained on/in chitosan after the second cross-linking were investigated by XPS analysis. As shown in Figure S4, the imprinted Pd(II) on/in chitosan maintained its species as $PdCl_4^{2-}$ in solutions with the pH at 7.5 and 12.5, while no peaks were observed at pH 14.5. This indicated that a solution pH of 7.5−12.5 of the second cross-linking was suitable for ICA preparation. Hence, pH 12.5 was chosen as the preferred second cross-linking pH to ensure good stability of the final adsorbent.

Furthermore, a multiple response method was employed to optimize the independent variables (ECH dosages used in first and second cross-linking, the imprinting pH value) and the response variable [Pd(II) selectivity] through Design Expert. The best local maximum was observed at 0.10% first cross-linking ECH, an imprinting pH of 1.0, and 1.00% second cross-linking ECH, corresponding to a Pd(II) selectivity coefficient of 116.97 with a desirability of 0.971, which demonstrated that the experimental model and desired conditions have been successfully represented by the estimated function.

Characterization of the Ion-Imprinted Chitosan Adsorbent. To gain insight into the functional groups responsible for Pd(II) imprinting, FTIR spectra of NICA (Figure 5a) and chitosan fibers after imprinting (Figure 5b) after second cross-linking (Figure 5c) and well-prepared ICA (Figure 5d) were analyzed. As shown in Figure 5a, the strong band at ∼3361 cm^{-1} showing overlapping of $-NH_2$ and −OH stretching vibrations could be assigned to the free amine and hydroxyl groups;[34,39] meanwhile, the bands at 1061 and 1026 cm^{-1} could be assigned to the C−N stretching vibration in amine groups.[40,41] However, as seen in Figure 5b, the band assigned to $-NH_2$ and −OH vibrations (∼3361 cm^{-1}) shifted to 3285 cm^{-1}, and the peaks attributed to the C−N vibration at 1061 and 1026 cm^{-1} overlapped into the peak at 1026 cm^{-1}, verifying that amine groups participated in Pd(II) imprinting. Additionally, the peak attributed to C−N vibrations maintained its position at 1026 cm^{-1} even after Pd(II) imprinting and second cross-linking (Figure 5c), indicating that the amine groups were maintained after imprinting with Pd(II) ions and cross-linking with ECH. The FTIR spectrum of the prepared ICA after Pd(II) elution with acidified thiourea is shown in Figure 5d, with the amine groups still unaffected, indicating that the imprinted Pd(II) ions were safely and fully eluted by the acidified thiourea solution without affecting the structure of the prepared ICA. Overall, the FTIR analysis verified that the

https://doi.org/10.1021/acsomega.1c00685
ACS Omega 2021, 6, 13057−13065

Table 4. Selectivity Coefficients of IR-120H, IR-900, IR-4200, NICA, and ICA for Pd(II)

adsorbents	IR-120H	IR-900	IR-4200	NICA	ICA
βPd/Co & βPd/Ni	NA	∞	∞	∞	∞
βPd/Pt	NA	0.34 ± 0.01	0.17 ± 0.04	9.06 ± 0.71	115.83 ± 0.02

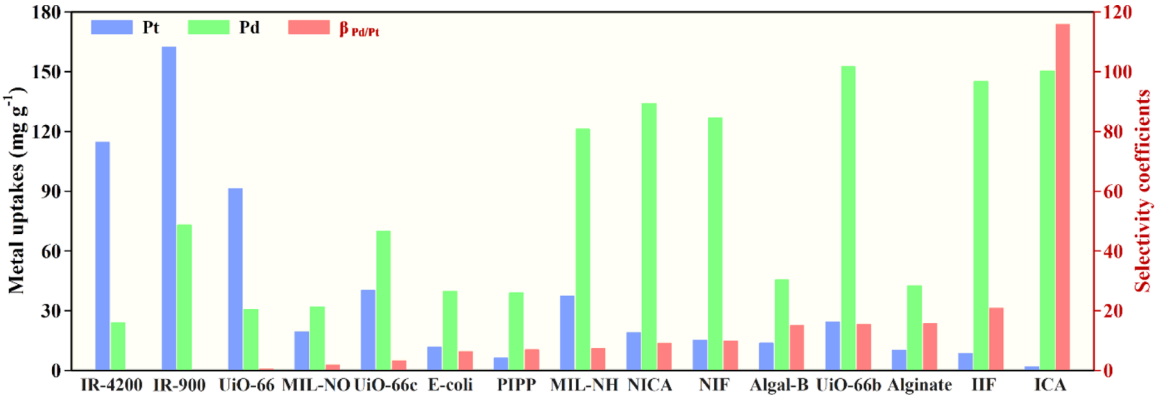

Figure 7. Comparison of the Pt(VI) and Pd(II) uptakes and selectivity for Pd on ICA and NICA with various adsorbents: IR-4200, IR-900, UiO-66,[42] MIL-101(Cr)-NO_2 (MIL-NO),[43] UiO-66-$NHCOCH_3$ (UiO-66c),[42] *Escherichia coli* biomass (*E-coli*),[44] Pd(II)-imprinted porous polymer particles (PIPP),[45] MIL-101(Cr)-NH_2 (MIL-NH),[43] non-imprinted chitosan fibers (NIFs),[16] algal-based beads (Algal-B),[46] UiO-66-NH_2 (UiO-66b),[42] alginate,[46] and ion-imprinted chitosan fibers (IIFs).[16]

amine groups in chitosan fibers were responsible for selectively adsorbing Pd(II).

Selective Adsorption Studies. The selective adsorption performance of the ICA synthesized under the optimal conditions as well as NICA, two industrial-grade strong-base anion-exchange resins with the quaternary ammonium group (IR-900 and IR-4200), and a strong-acid cation-exchange resin with the sulfonic group (IR-120H) were evaluated and compared through competitive adsorption experiments in multiple-metal solutions. As shown in Figure 6, the Pd(II) uptake was as high as 150.30 ± 0.03 mg g^{-1}; meanwhile, the Pt(IV) uptake was negligible (3.00 ± 2.07 mg g^{-1}) in the case of ICA. The other competing ions like Co(II) and Ni(II) were, however, not adsorbed by ICA. This indicates that ICA was a highly selective adsorbent toward Pd(II) ions in the midst of the competing ions. By comparison, the adsorption capacity of ICA for Pt(IV) was markedly lower than those for IR-900, IR-4200, and NICA. It could thus be noted that although Pt(IV) ions ($PtCl_6^{2-}$) are the main competing metallic ions whose species are similar to the Pd(II) ions ($PdCl_4^{2-}$) in the acidic solution, the adsorption was inhibited due to the fixed cavities created for Pd(II) by the imprinting and cross-linking steps. The uptakes of Co(II) and Ni(II) cations (Co^{2+} and Ni^{2+}) on all adsorbents were negligible, with the exception of IR-120H, the reason being the inherently strongly acidic IR-120H cation-exchange resin. The Pd(II) selectivity coefficients ($\beta_{Pd/Co}$, $\beta_{Pd/Ni}$, and $\beta_{Pd/Pt}$) toward Co(II), Ni(II), and Pt(IV) ions are shown in Table 4. The $\beta_{Pd/Pt}$ values of IR-120H, IR-900, IR-4200, and NICA were less than one-tenth that of ICA, indicating the remarkable selectivity of ICA for Pd(II) compared with these industrial-grade resins and the chitosan adsorbent without imprinting. Consequently, a markedly higher $\beta_{Pd/Pt}$ of 115.83 was obtained for the ICA, which is close to the predicted Pd(II) selectivity (116.97), indicating that the Box−Behnken design using the desirability functions could be used to develop a high-selective-performance adsorbent. Furthermore, the selectivity coefficients for Pd(II) ($\beta_{Pd/Pt}$) and Pd(II) uptakes of ICA prepared under optimal conditions were compared among various adsorbents (Figure 7), including our previous work of an ion-imprinted adsorbent without using RSM for optimizing the preparation conditions, metal−organic frameworks, biosorbents, etc. This indicated the extraordinary Pd(II) selectivity and uptake of ICA among the reported selective adsorbents.

Regeneration of Pd(II)-Loaded ICA. After adsorption of Pd(II) onto 0.04 g of ICA in 100 mL containing 200 mg L^{-1}, the Pd(II)-loaded ICA was regenerated by desorption using 40 mL of acidic thiourea solution (0.2 M thiourea/0.05 M HCl) and then rinsed twice with 40 mL of NaOH solution (0.1 M) and distilled water. The regenerated ICA was reused in the subsequent adsorption cycles. As shown in Figure S5, the loaded Pd(II) was completely eluted from ICA, and the stable adsorption performance of the ICA was maintained up to five cycles of adsorption and desorption, indicating the excellent reusability and stability of ICA.

CONCLUSIONS

The highly acid-tolerant Pd(II)-selective adsorbent was developed, and its preparation method was successfully optimized by the Box−Behnken design. The dosage of ECH used in two steps of cross-linking and the pH of the imprinting reaction medium, which were the dominance for synthesizing an ion-imprinting chitosan adsorbent, were chosen as factors in a three-level factorial Box−Behnken design. RSM successfully verified the effect of these dominant factors on the adsorbent's selectivity. The optimal conditions were determined as 0.10% first cross-linking ECH, an imprinting pH of 1.0, and 1.00% second cross-linking ECH on the basis of 2.0 g of formed chitosan fibers with a predicted maximum selectivity coefficient ($\beta_{Pd/Pt}$) of 116.97. Hereafter, these optimal conditions were employed to prepare the ion-imprinted chitosan adsorbent, and the Pd(II) selectivity coefficient of ICA ($\beta_{Pd/Pt}$: 115.83) was evaluated and compared with that of the chitosan adsorbent without imprinting and other various adsorbents, indicating the extraordinary Pd(II) selectivity on ICA among the reported selective adsorbents.

https://doi.org/10.1021/acsomega.1c00685
ACS Omega 2021, 6, 13057−13065

■ ASSOCIATED CONTENT

Supporting Information

The Supporting Information is available free of charge at https://pubs.acs.org/doi/10.1021/acsomega.1c00685.

Additional data of Box−Behnken experimental design, equilibrium diagrams for Pd(II) solutions, XPS Pd 3d spectra, and adsorption and desorption cycles (PDF)

■ AUTHOR INFORMATION

Corresponding Authors

Myung-Hee Song − *School of Chemical Engineering, Jeonbuk National University, Jeonbuk 54896, Republic of Korea*; Phone: +82-63-270-2308; Email: bsbsmh@gmail.com; Fax: +82-63-270-2306

Yeoung-Sang Yun − *School of Chemical Engineering, Jeonbuk National University, Jeonbuk 54896, Republic of Korea*; orcid.org/0000-0002-2583-8278; Phone: +82-63-270-2308; Email: ysyun@jbnu.ac.kr; Fax: +82-63-270-2306

Authors

Shuo Lin − *School of Chemical Engineering, Jeonbuk National University, Jeonbuk 54896, Republic of Korea; Department of Chemistry, University of Calgary, Calgary, Alberta T2N 1N4, Canada*

Wei Wei − *School of Chemical Engineering, Jeonbuk National University, Jeonbuk 54896, Republic of Korea; Key Laboratory for Synergistic Prevention of Water and Soil Environmental Pollution, Xinyang Normal University, Xinyang, Henan 464000, China*

Xiaoyu Lin − *School of Chemical Engineering, Jeonbuk National University, Jeonbuk 54896, Republic of Korea*

John Kwame Bediako − *School of Chemical Engineering, Jeonbuk National University, Jeonbuk 54896, Republic of Korea*

D. Harikishore Kumar Reddy − *School of Chemical Engineering, Jeonbuk National University, Jeonbuk 54896, Republic of Korea*; orcid.org/0000-0002-3180-4314

Complete contact information is available at: https://pubs.acs.org/10.1021/acsomega.1c00685

Notes

The authors declare no competing financial interest.

■ ACKNOWLEDGMENTS

This work was financially supported by the South Korean Government through the NRF (2020R1A2C3009769) grant and the National Natural Science Foundation of China (51808477).

■ REFERENCES

(1) Lanaridi, O.; Sahoo, A. R.; Limbeck, A.; Naghdi, S.; Eder, D.; Eitenberger, E.; Csendes, Z.; Schnürch, M.; Bica-Schröder, K. Toward the Recovery of Platinum Group Metals from a Spent Automotive Catalyst with Supported Ionic Liquid Phases. *ACS Sustainable Chem. Eng.* **2021**, *9*, 375−386.

(2) Nguyen, V. T.; Riaño, S.; Aktan, E.; Deferm, C.; Fransaer, J.; Binnemans, K. Solvometallurgical Recovery of Platinum Group Metals from Spent Automotive Catalysts. *ACS Sustainable Chem. Eng.* **2020**, *9*, 337−350.

(3) Lin, S.; Bediako, J. K.; Song, M.-H.; Kim, J.-A.; Cho, C.-W.; Zhao, Y.; Choi, J.-W.; Yun, Y.-S. Effective Recovery of Pt(IV) from Acidic Solution by a Defective Metal−Organic Frameworks Using Central Composite Design for Synthesis. *ACS Sustainable Chem. Eng.* **2019**, *7*, 7510−7518.

(4) Islam, A.; Ahmed, T.; Awual, M. R.; Rahman, A.; Sultana, M.; Aziz, A. A.; Monir, M. U.; Teo, S. H.; Hasan, M. Advances in sustainable approaches to recover metals from e-waste-A review. *J. Cleaner Prod.* **2020**, *244*, 118815.

(5) Ding, Y.; Zhang, S.; Liu, B.; Zheng, H.; Chang, C.-c.; Ekberg, C. Recovery of precious metals from electronic waste and spent catalysts: A review. *Resour., Conserv. Recycl.* **2019**, *141*, 284−298.

(6) Dong, H.; Zhao, J.; Chen, J.; Wu, Y.; Li, B. Recovery of platinum group metals from spent catalysts: A review. *Int. J. Miner. Process.* **2015**, *145*, 108−113.

(7) Ravi Kumar, M. N. V. A review of chitin and chitosan applications. *React. Funct. Polym.* **2000**, *46*, 1−27.

(8) Varma, A. J.; Deshpande, S. V.; Kennedy, J. F. Metal complexation by chitosan and its derivatives: a review. *Carbohydr. Polym.* **2004**, *55*, 77−93.

(9) Thakur, V. K.; Thakur, M. K. Recent Advances in Graft Copolymerization and Applications of Chitosan: A Review. *ACS Sustainable Chem. Eng.* **2014**, *2*, 2637−2652.

(10) Guibal, E. Interactions of metal ions with chitosan-based sorbents: a review. *Sep. Purif. Technol.* **2004**, *38*, 43−74.

(11) Mincke, S.; Asere, T. G.; Verheye, I.; Folens, K.; Vanden Bussche, F.; Lapeire, L.; Verbeken, K.; Van Der Voort, P.; Tessema, D. A.; Fufa, F.; Du Laing, G.; Stevens, C. V. Functionalized chitosan adsorbents allow recovery of palladium and platinum from acidic aqueous solutions. *Green Chem.* **2019**, *21*, 2295−2306.

(12) Vakili, M.; Deng, S.; Li, T.; Wang, W.; Wang, W.; Yu, G. Novel crosslinked chitosan for enhanced adsorption of hexavalent chromium in acidic solution. *Chem. Eng. J.* **2018**, *347*, 782−790.

(13) Kong, D.; Wang, N.; Qiao, N.; Wang, Q.; Wang, Z.; Zhou, Z.; Ren, Z. Facile Preparation of Ion-Imprinted Chitosan Microspheres Enwrapping Fe3O4 and Graphene Oxide by Inverse Suspension Cross-Linking for Highly Selective Removal of Copper(II). *ACS Sustainable Chem. Eng.* **2017**, *5*, 7401−7409.

(14) He, J.; Shang, H.; Zhang, X.; Sun, X. Synthesis and application of ion imprinting polymer coated magnetic multi-walled carbon nanotubes for selective adsorption of nickel ion. *Appl. Surf. Sci.* **2018**, *428*, 110−117.

(15) Yu, Q.; Deng, S.; Yu, G. Selective removal of perfluorooctane sulfonate from aqueous solution using chitosan-based molecularly imprinted polymer adsorbents. *Water Res.* **2008**, *42*, 3089−3097.

(16) Lin, S.; Wei, W.; Wu, X.; Zhou, T.; Mao, J.; Yun, Y.-S. Selective recovery of Pd(II) from extremely acidic solution using ion-imprinted chitosan fiber: Adsorption performance and mechanisms. *J. Hazard. Mater.* **2015**, *299*, 10−17.

(17) Velempini, T.; Pillay, K.; Mbianda, X. Y.; Arotiba, O. A. Carboxymethyl cellulose thiol-imprinted polymers: Synthesis, characterization and selective Hg(II) adsorption. *J. Environ. Sci.* **2019**, *79*, 280−296.

(18) Liu, P.; An, H.; Ren, Y.; Feng, J.; Ma, J. Selective recognition mechanism of molybdenum(VI) ions binding onto ion-imprinted particle in the water. *Chem. Eng. J.* **2018**, *349*, 176−183.

(19) Yang, S.; Xu, M.; Yin, J.; Zhao, T.; Li, C.; Hua, D. Thermal-responsive Ion-imprinted magnetic microspheres for selective separation and controllable release of uranium from highly saline radioactive effluents. *Sep. Purif. Technol.* **2020**, *246*, 116917.

(20) Monier, M.; Abdel-Latif, D. A.; Abou El-Reash, Y. G. Ion-imprinted modified chitosan resin for selective removal of Pd(II) ions. *J. Colloid Interface Sci.* **2016**, *469*, 344−354.

(21) Wang, J.; Li, Z. Enhanced selective removal of Cu(II) from aqueous solution by novel polyethylenimine-functionalized ion imprinted hydrogel: Behaviors and mechanisms. *J. Hazard. Mater.* **2015**, *300*, 18−28.

(22) Davarnejad, R.; Panahi, P. Cu (II) removal from aqueous wastewaters by adsorption on the modified Henna with Fe3O4 nanoparticles using response surface methodology. *Sep. Purif. Technol.* **2016**, *158*, 286−292.

(23) Myers, R. H. *Response Surface Methodology: Process and Product Optimization Using Designed Experiments*; John Wiley & Sons: New York, 1991.
(24) Dastyar, W.; Zhao, M.; Yuan, W.; Li, H.; Ting, Z. J.; Ghaedi, H.; Yuan, H.; Li, X.; Wang, W. Effective Pretreatment of Heavy Metal-Contaminated Biomass Using a Low-Cost Ionic Liquid (Triethylammonium Hydrogen Sulfate): Optimization by Response Surface Methodology−Box Behnken Design. *ACS Sustainable Chem. Eng.* **2019**, *7*, 11571−11581.
(25) Ferreira, S. L. C.; Bruns, R. E.; Ferreira, H. S.; Matos, G. D.; David, J. M.; Brandão, G. C.; da Silva, E. G. P.; Portugal, L. A.; dos Reis, P. S.; Souza, A. S.; dos Santos, W. N. L. Box-Behnken design: An alternative for the optimization of analytical methods. *Anal. Chim. Acta* **2007**, *597*, 179−186.
(26) Liu, J.; Su, D.; Yao, J.; Huang, Y.; Shao, Z.; Chen, X. Soy protein-based polyethylenimine hydrogel and its high selectivity for copper ion removal in wastewater treatment. *J. Mater. Chem. A* **2017**, *5*, 4163−4171.
(27) Ren, Y.-M.; Yang, J.; Ma, W.-Q.; Ma, J.; Feng, J.; Liu, X.-L. The selective binding character of a molecular imprinted particle for Bisphenol A from water. *Water Res.* **2014**, *50*, 90−100.
(28) Li, H.; Gan, S.; Han, D.; Ma, W.; Cai, B.; Zhang, W.; Zhang, Q.; Niu, L. High performance Pd nanocrystals supported on SnO2-decorated graphene for aromatic nitro compound reduction. *J. Mater. Chem. A* **2014**, *2*, 3461−3467.
(29) Wang, H.-F.; Ariga, H.; Dowler, R.; Sterrer, M.; Freund, H.-J. Surface science approach to catalyst preparation − Pd deposition onto thin Fe_3O_4(111) films from $PdCl_2$ precursor. *J. Catal.* **2012**, *286*, 1−5.
(30) Darabdhara, G.; Das, M. R.; Turcheniuk, V.; Turcheniuk, K.; Zaitsev, V.; Boukherroub, R.; Szunerits, S. Reduced graphene oxide nanosheets decorated with AuPd bimetallic nanoparticles: a multi-functional material for photothermal therapy of cancer cells. *J. Mater. Chem. B* **2015**, *3*, 8366−8374.
(31) Chenakin, S. P.; Melaet, G.; Szukiewicz, R.; Kruse, N. XPS study of the surface chemical state of a Pd/(SiO_2+TiO_2) catalyst after methane oxidation and SO_2 treatment. *J. Catal.* **2014**, *312*, 1−11.
(32) Wagner, C. D.; Riggs, W. M.; Davis, L. E.; Moulder, J. F.; Muilenberg, G. E. *Handbook of X-ray Photoelectron Spectroscopy: A Reference Book of Standard Data for Use in X-ray Photoelectron Spectroscopy*; PerkinElmer Corporation, 1979.
(33) Lin, S.; Zhao, Y.; Bediako, J. K.; Cho, C.-W.; Sarkar, A. K.; Lim, C.-R.; Yun, Y.-S. Structure-controlled recovery of palladium(II) from acidic aqueous solution using metal-organic frameworks of MOF-802, UiO-66 and MOF-808. *Chem. Eng. J.* **2019**, *362*, 280−286.
(34) Lin, S.; Kumar Reddy, D. H.; Bediako, J. K.; Song, M.-H.; Wei, W.; Kim, J.-A.; Yun, Y.-S. Effective adsorption of Pd(ii), Pt(iv) and Au(iii) by Zr(iv)-based metal−organic frameworks from strongly acidic solutions. *J. Mater. Chem. A* **2017**, *5*, 13557−13564.
(35) Ivashenko, O.; van Herpt, J. T.; Feringa, B. L.; Browne, W. R.; Rudolf, P. Rapid reduction of self-assembled monolayers of a disulfide terminated para-nitrophenyl alkyl ester on roughened Au surfaces during XPS measurements. *Chem. Phys. Lett.* **2013**, *559*, 76−81.
(36) Liu, H.; Yang, F.; Zheng, Y.; Kang, J.; Qu, J.; Chen, J. P. Improvement of metal adsorption onto chitosan/Sargassum sp. composite sorbent by an innovative ion-imprint technology. *Water Res.* **2011**, *45*, 145−154.
(37) Chen, S.; Yau, S.; Fan, L.; Yang, Y. In situ STM and ex situ XPS examination of the adsorption and polymerization of metanilic acid and aniline on Au(111) electrode. *J. Electroanal. Chem.* **2014**, *716*, 150−157.
(38) Mao, J.; Lee, S. Y.; Won, S. W.; Yun, Y.-S. Surface modified bacterial biosorbent with poly(allylamine hydrochloride): Development using response surface methodology and use for recovery of hexachloroplatinate(IV) from aqueous solution. *Water Res.* **2010**, *44*, 5919−5928.
(39) Wang, J.-P.; Chen, Y.-Z.; Yuan, S.-J.; Sheng, G.-P.; Yu, H.-Q. Synthesis and characterization of a novel cationic chitosan-based flocculant with a high water-solubility for pulp mill wastewater treatment. *Water Res.* **2009**, *43*, 5267−5275.
(40) Won, S. W.; Kim, S.; Kotte, P.; Lim, A.; Yun, Y.-S. Cationic polymer-immobilized polysulfone-based fibers as high performance sorbents for Pt(IV) recovery from acidic solutions. *J. Hazard. Mater.* **2013**, *263*, 391−397.
(41) Lawrie, G.; Keen, I.; Drew, B.; Chandler-Temple, A.; Rintoul, L.; Fredericks, P.; Grøndahl, L. Interactions between Alginate and Chitosan Biopolymers Characterized Using FTIR and XPS. *Biomacromolecules* **2007**, *8*, 2533−2541.
(42) Lin, S.; Bediako, J. K.; Cho, C.-W.; Song, M.-H.; Zhao, Y.; Kim, J.-A.; Choi, J.-W.; Yun, Y.-S. Selective adsorption of Pd(II) over interfering metal ions (Co(II), Ni(II), Pt(IV)) from acidic aqueous phase by metal-organic frameworks. *Chem. Eng. J.* **2018**, *345*, 337−344.
(43) Lim, C.-R.; Lin, S.; Yun, Y.-S. Highly efficient and acid-resistant metal-organic frameworks of MIL-101(Cr)-NH2 for Pd(II) and Pt(IV) recovery from acidic solutions: Adsorption experiments, spectroscopic analyses, and theoretical computations. *J. Hazard. Mater.* **2020**, *387*, 121689.
(44) Kim, S.; Song, M.-H.; Wei, W.; Yun, Y.-S. Selective biosorption behavior of Escherichia coli biomass toward Pd(II) in Pt(IV)−Pd(II) binary solution. *J. Hazard. Mater.* **2015**, *283*, 657−662.
(45) Jiang, Y.; Kim, D. Synthesis and selective adsorption behavior of Pd(II)-imprinted porous polymer particles. *Chem. Eng. J.* **2013**, *232*, 503−509.
(46) Wang, S.; Vincent, T.; Roux, J.-C.; Faur, C.; Guibal, E. Pd(II) and Pt(IV) sorption using alginate and algal-based beads. *Chem. Eng. J.* **2017**, *313*, 567−579.

https://doi.org/10.1021/acsomega.1c00685
ACS Omega 2021, 6, 13057−13065